Geomechanics and Engineering, *Vol. 43, No. 3 (2025) 227-242*
https://doi.org/10.12989/gae.2025.43.3.227

Prediction of transportation volume loss by earthquake in railway network based on functionality loss curves and OD matrix method

Jiyun Jeon[1], Mintaek Yoo*[1] and Ji Hyeon Kim**[2]

[1]*Department of Civil and Environmental Engineering, Gachon University, South Korea*
[2]*Advanced Railroad Civil Engineering Division, Korea Railroad Research Institute, South Korea*

(*Received May 19, 2025, Revised September 24, 2025, Accepted October 22, 2025*)

Abstract. This study proposes a methodology for predicting the extent of transportation loss in a newly developed railway network during seismic events. In this process, a direct estimation method for the OD (Origin-Destination) matrix was employed to derive the population movement ratio for each railway line, which was then used to estimate the approximate volume of transported population across the railway network. The transportation volume was estimated using the actual boarding and alighting data from a railway line in Seoul and a destination-based OD Matrix model. Next, the functionality loss of each structural component in the railway network was derived by integrating seismic fragility curves with restoration curves. The functionality loss of individual railway infrastructure components was evaluated for earthquake magnitudes $M_L = 6$ and $M_L = 7$, using the Korean ground motion attenuation equation, epicentral distance, and short-period amplification factors. Subsequently, the overall average functionality loss of the railway network was calculated by incorporating the functionality loss and length of each railway line. For a more conservative assessment, the maximum functionality loss within each segment was also considered. As a result, for an earthquake with magnitude $M_L = 6$, the transportation loss of the simulated railway network was estimated to be 7.65% when reflecting the average functionality loss, and 15.13% when reflecting the maximum functionality loss. Subsequently, under an $M_L = 7$ earthquake scenario, the transportation loss for the simulated railway network was predicted to be 19.37% when reflecting average functionality loss and 30.14% when reflecting maximum functionality loss.

Keywords: earthquake; fragility curve; functionality loss; OD Matrix; transportation volume loss

1. Introduction

Earthquakes are disasters that impose direct loads on structures and have historically caused significant loss of life and property. In South Korea, the occurrence of moderate or greater magnitude earthquakes has been increasing in recent years, including the 2016 Gyeongju earthquake ($M_L = 5.8$), the 2017 Pohang earthquake ($M_L = 5.4$), and the 2024 Buan earthquake ($M_L = 4.8$). These recent seismic events have raised awareness that the Korean Peninsula can no longer be considered a seismically safe zone, thereby underscoring the growing need for research on earthquake preparedness and damage prediction. In particular, the railway network, as a key component of national transportation infrastructure, plays a critical role in both population mobility and transportation. Its significance continues to grow with the expansion of railway structures and the increasing volume of population transportation. If these railway structures experience collapse or disruptions in transportation movement due to seismic events, substantial socio-economic losses may occur.

In response, it is necessary to prepare for potential losses in railway transportation volume caused by earthquakes. Numerous studies have thus focused on estimating transportation capacity within railway networks and evaluating functionality degradation in structural components such as embankments, bridges, and tunnels.

In previous studies on railway network transportation analysis, Yang *et al*. (2018) utilized the PAPTOR algorithm to calculate public transportation accessibility, quantifying time losses between OD(Origin-Destination) pairs as potential improvements and confirming that route improvement priorities can be identified through station-level OD analysis. Choi (2008) developed a mathematical model to estimate traffic volumes on unobserved links, thereby enhancing the reliability of OD matrix estimations even with limited traffic data. Lee and Lee (2023) utilized the Migration Effectiveness Index (MEI), which offers greater conceptual validity than the Net Migration Rate (NMR), to assess the imbalance in population movement and its impact on population redistribution. Building on previous studies that used OD matrices for restoration prioritization and population redistribution, this study applied the OD matrix method to identify population proportions for each railway line.

Subsequently, numerous studies have addressed the

*Corresponding author, Assistant Professor
E-mail: mintaekyoo@gachon.ac.kr
**Corresponding author, Senior Researcher
E-mail: jhkim06@krri.re.kr
[a]Graduate student

ISSN: 2005-307X (Print), 2092-6219 (Online)

structural components of railway networks, such as railway bridges, embankments, and tunnels. Kim *et al*. (2023) proposed seismic fragility functions for bridges, tunnels, and embankments based on damage states and used restoration curves to derive the expected damage rates and recovery times for the railway network. Yoo *et al*. (2025) quantified the overall transportation loss in a railway network by integrating seismic fragility curves with OD matrix-based analysis. This study is similar to the present work in that it quantitatively evaluated transportation loss in railway networks using the OD matrix. Liu *et al.* (2018) confirmed that metro tunnels constructed in faulted ground are subject to non-uniform settlement and increased structural vulnerability under seismic loading. Kurian *et al.* (2006) derived fragility curves through pushover and nonlinear dynamic analyses, confirming sensitivity differences at higher damage levels depending on structural modeling methods. Yoo and Hong (2024) evaluated seismic risk of an underground railway station using fragility curves, confirming that deeper and softer ground conditions lead to higher structural damage. Yang *et al*. (2020) proposed a set of seismic fragility curves to quantitatively assess the vulnerability of high-speed railway lines based on observed earthquake damage data. Wei *et al.* (2017) evaluated the nonlinear behavior of friction-based fixed bearings used in high-speed railway continuous bridges and found that lower friction coefficients increase bearing damage but enhance protection for other components. Guo *et al*. (2019) assessed the seismic performance of 22 single piers in Chinese high-speed railway bridges through pushover analysis and found that tall piers exhibited better seismic performance and ductility. Wang *et al.* (2014) evaluated the seismic fragility of E-shaped dampers and bearings applied to high-speed railway bridges in southwestern China, confirming that bearing components were more vulnerable to damage than piers. Wei et al. (2020) assessed the effectiveness of seismic fragility analysis using artificial ground motions applied to continuous high-speed railway bridges, and confirmed that these motions could be practically utilized, given their similarity to real earthquake responses. Argyroudis and Kaynia (2015) evaluated the seismic stability of highway embankments and cut slopes. As a result, fragility curves were developed under various ground conditions, confirming that embankments are generally more vulnerable to seismic loads than cut slopes. In case of underground structure, structures embedded in soft ground are tend to exhibit greater seismic response amplification (Kwon *et al*. 2020, Yoo *et al*. 2022). In addition, Kwon *et al*. (2024) conducted dynamic numerical analyses using PLAXIS 2D to assess the seismic risk of subway structures in Korea. The results confirmed that seismic damage increases with deeper and softer ground conditions, and that long-period ground motions have a greater impact on structures than short-period ground motions. Andreotti and Lai (2019) developed fragility curves for mountain tunnels using fully nonlinear dynamic analyses, demonstrating that PGV/Vs30 reduces variability in fragility assessment due to site conditions. Nguyen *et al*. (2019) analyzed the seismic fragility of cut-and-cover subway tunnels and confirmed that fragility curves based on PGA/Vs30 are more stable and less sensitive to ground conditions compared to those based on PGA (Peak Ground Acceleration) or PGV (Peak Ground Velocity) alone. Avanaki *et al*. (2018) evaluated the seismic fragility of steel fiber reinforced concrete (SFRC) segment tunnel linings, demonstrating that hybrid SFRCs with high fiber content provide superior seismic resistance and ductility compared to conventional reinforced concrete. Park *et al*. (2019) developed seismic fragility curves for double-box underground tunnels through pushover analysis and found that PGV/Vs30 is a more reliable IM than PGA, with higher ground stiffness improving seismic performance. Yang *et al.* (2024) applied dynamic analysis to derive seismic fragility curves and verified that the resulting functions better represent the ground conditions and structural features specific to Korea. Huang *et al.* (2022) quantified tunnel restoration times by integrating fragility functions and recovery models under various earthquake scenarios and ground conditions. However, previous studies have mainly focused on analyzing seismic fragility curves for bridges, embankments, and tunnels under various ground conditions, or on addressing route improvement priorities and demographic imbalances caused by population movements. In contrast, research on the socioeconomic impacts and damage assessment associated with transportation capacity loss due to earthquakes remains limited. Accordingly, this study proposes the methodology for quantitatively analyzing the loss of transport capacity in railway networks caused by earthquakes. To quantitatively assess transport capacity, population-based transport volume was first analyzed using the OD matrix. Subsequently, the seismic functionality loss of railway structural components was evaluated through functionality loss curves derived from seismic fragility functions and restoration curves. Finally, a methodology combining the two concepts was proposed to predict transportation loss in the railway network, and its applicability was validated through application to a hypothetical network.

2. Methodology

This study estimated line-specific transportation volumes using the OD matrix and station-level boarding and alighting data. Functionality loss curves were then derived by integrating seismic fragility and restoration curves for railway structural components. Finally, transportation losses for each line were predicted by combining line-specific volumes with component functionality losses. The conceptual framework of this study is illustrated in Fig. 1.

2.1 Transportation volume prediction based on OD (Origin-Destination) matrix

An OD (Origin-Destination) matrix is a two-dimensional matrix commonly used in transportation and logistics to represent the flow of trips or transportation between origins and destinations within a specific region. Each row corresponds to an origin, and each column

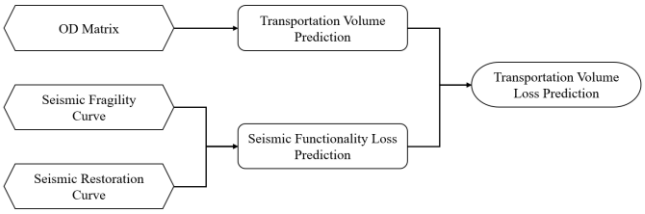

Fig. 1 Analytical Framework for transportation volume loss

corresponds to a destination. It is widely utilized in the field of transportation to quantitatively analyze movement patterns, and it plays a fundamental role in enhancing logistics efficiency through applications such as congestion analysis, public transportation route planning, optimization of vehicle routing, and freight transit time reduction. The segment-wise transportation volume based on the OD Matrix is given by Eq. (1).

$$OD_{ij} = \frac{Boarding_i \times Alighting_j}{\sum Alighting} \quad [person/day] \quad (1)$$

In this formula, "$Boarding$" denotes the quantity of passengers or freight embarking at origin zone i, while "$Alighting$" refers to the quantity disembarking at destination zone j. "$\sum Alighting$" represents the total number of alightings, serving as an indirect indicator of the spatial distribution of major activity centers within the actual population. Using this destination-based model derived from the OD Matrix, the transportation volume of the railway network was quantitatively evaluated.

2.2 Seismic functionality loss prediction for railway structure component

The railway network consists of structural components such as embankments, bridges, and tunnels. These railway structural components possess distinct ground conditions and structural characteristics. When an earthquake occurs, in the case of bridges, seismic loads generated during earthquakes propagate from the foundation components to the superstructure. In the case of tunnels, seismic response depends significantly on interaction with surrounding ground conditions, and is influenced by factors such as burial depth and cross-sectional geometry. Embankment structures tend to amplify seismic waves as they propagate through the ground, due to the geotechnical properties of the soil. In addition, repeated shaking may lead to a reduction in shear strength within the embankment body. These structural differences lead to significant variations in seismic load transmission and functionality degradation, depending on seismic wave amplification associated with ground conditions and embedment depth.

Therefore, to develop a model capable of predicting the overall functionality loss of a railway network, it is essential to establish functionality loss curves for the key structural components—bridges, embankments, and tunnels. For this purpose, seismic fragility curves were established to evaluate the seismic performance of each railway structural component, and restoration curves were constructed to capture their functionality over time. In addition, the recovery period for the railway network was set to 100 days, based on prior studies showing that the functionality of components in severely damaged states increases significantly around the 100-day mark on the restoration curve. These elements were then integrated into a comprehensive model for analyzing overall functionality loss.

The seismic functionality curve can be derived by integrating seismic fragility curves with restoration curves, enabling the prediction of structural functionality over time during the recovery process. During this process, the recovery time varies depending on the structural characteristics of each component, such as bridges, embankments, and tunnels.

The seismic functionality loss curve, derived from the seismic functionality curve, offers a predictive measure of structural functionality loss under specific seismic intensities, serving as a critical tool for anticipating and preparing for future earthquake events.

2.2.1 Seismic fragility curve

A seismic fragility curve represents the probability of exceedance for a specific damage state of a railway structural component under a given seismic intensity.

Seismic fragility curves can be derived through numerical or empirical methods. The numerical approach involves applying ground motions of varying intensities, which may include recorded or synthetic earthquake records. In contrast, the empirical approach estimates damage probabilities by analyzing observed damage data from past earthquake events.

In this study, a linear weighted combination formula and prior numerical studies were utilized to derive seismic fragility curves for assessing the functionality loss of a newly proposed railway network. The damage states for each railway structural components are classified into five levels: none (ds_0), minor state (ds_1), moderate state (ds_2), extensive state (ds_3), and complete state (ds_4). The seismic fragility curve in Eq. (2) is expressed as a cumulative distribution function (CDF), indicating the probability of exceeding a given damage state (ds_i) under an intensity measure (IM).

$$P[ds_i|IM] = \Phi\left(\frac{lnX - \mu}{\beta}\right), \quad i = 0, 1, 2, 3, 4 \quad (2)$$

In this formula, $P[ds_i|IM]$ denotes the probability of exceeding a given damage state at a ground motion intensity (IM), $\Phi(\cdot)$ represents the cumulative distribution function of the standard normal distribution, μ is the mean of lnX, and β is the standard deviation of lnX.

The seismic fragility curves for bridges were derived based on the study by Kim *et al.* (2023). For embankment sections, the fragility curves were developed with reference to the work of Argyroudis and Kaynia (2015), while the data for tunnel fragility curves were adopted from the study by Kwon *et al.* (2024). The seismic fragility functions for bridges, embankments, and tunnels are presented in Table 1, Tables 2 and 3, respectively. The seismic fragility curve for bridges is illustrated in Fig. 2.

Table 1 Seismic fragility curve for bridge, data: Kim *et al.* (2023)

Damage State	Median (μ)	Standard Deviation (β)
Minor	0.293	0.632
Moderate	0.464	0.677
Extensive	0.596	0.699
Complete	0.853	0.691

Table 2 Seismic fragility curve for embankment, data: Argyroudis and Kaynia (2015)

	Damage State	Median (μ)	Standard Deviation (β)
Soft ground (H=6 m)	Minor	0.12	0.80
	Moderate	0.20	
	Extensive	0.34	
Soft ground (H=4 m)	Minor	0.25	0.80
	Moderate	0.37	
	Extensive	0.54	
Soft ground (H=2 m)	Minor	0.40	0.80
	Moderate	0.53	
	Extensive	0.72	
	Damage State	Median (μ)	Standard Deviation (β)
Stiff ground (H=6 m)	Minor	0.30	0.70
	Moderate	0.50	
	Extensive	0.84	
Stiff ground (H=4 m)	Minor	0.36	0.70
	Moderate	0.57	
	Extensive	0.91	
Stiff ground (H=2 m)	Minor	0.52	0.70
	Moderate	0.77	
	Extensive	1.77	

Table 3 Seismic fragility curve for tunnel, data: Kwon *et al.* (2024)

	Damage State	Median (μ)	Standard Deviation (β)
Shallow Tunnel (below 20 m)	Minor	0.296	0.619
	Moderate	0.327	
	Extensive	0.531	
Deep Tunnel (above 20 m)	Minor	0.130	0.485
	Moderate	0.293	
	Extensive	0.449	

2.2.2 Seismic restoration curve

A seismic restoration curve is a curve that quantitatively represents the level of functionality of a structure over time following an earthquake. The seismic restoration curve provides a quantitative measure of the time required for a railway structural component to recover its full functionality, and is an important tool for planning disaster response and understanding how quickly the structure can return to normal. Deriving the seismic restoration curve using the following formula

$$Q[ds_i|t] = \Phi\left(\frac{lnY - \delta}{\gamma}\right), \quad i = 0, 1, 2, 3, 4 \tag{3}$$

In this formula, $Q[ds_i|t]$ represents the probability of restoration for each damage state over time, and t denotes the restoration evaluation period. $\Phi(\cdot)$ is the cumulative distribution function of the standard normal distribution, δ is the mean of the lognormal distribution indicating the restoration time, and γ is the standard deviation reflecting the uncertainty of restoration time.

To derive the seismic restoration curves for each railway structure component, the average recovery times and recovery rates for each damage state were applied based on the restoration data provided by Yoo *et al.* (2025). The seismic restoration curves for bridges, embankments and tunnels in the railway network are provided in Table 4., and the restoration curve for bridges is shown in Fig. 3.

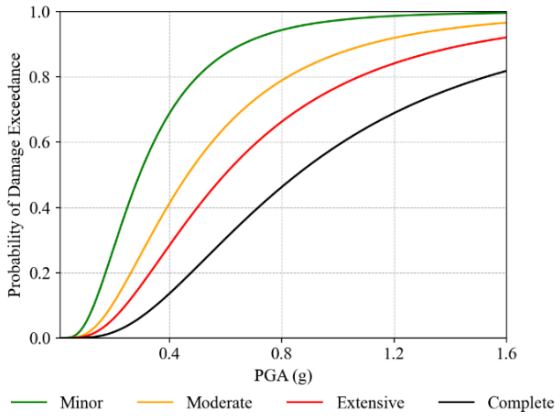

Fig. 2 Seismic fragility curve for bridge

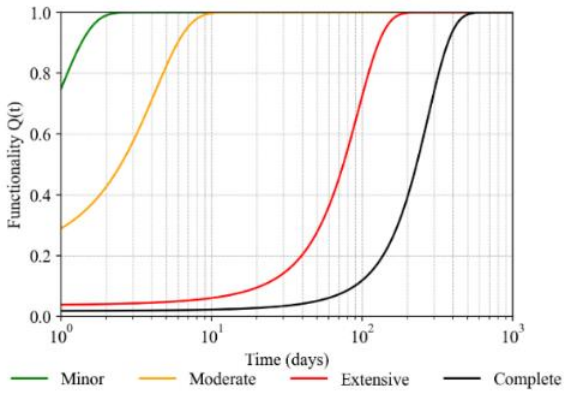

Fig. 3 Seismic restoration curve for bridge

2.2.3 Seismic functionality loss curve

A seismic functionality curve is a curve that quantitatively evaluates the degradation in structural functionality caused by an earthquake, as a function of

Table 4 Seismic restoration curve for railway network, data: Yoo *et al*. (2025)

	Damage State	Median (δ)	Standard Deviation (γ)
Bridge	Minor	0.6	0.6
	Moderate	2.5	2.7
	Extensive	75	42
	Complete	230	110
	Damage State	Median (δ)	Standard Deviation (γ)
Embankment	Minor	0.9	0.07
	Moderate	3.3	3
	Extensive	40	29
	Damage State	Median (δ)	Standard Deviation (γ)
Tunnel	Minor	0.5	0.3
	Moderate	2.4	2
	Extensive	45	30

seismic intensity. It serves as a key indicator for assessing the seismic resilience of railway networks and determining their operational availability. Deriving the seismic functionality curve using the following formula proposed by Huang *et al*. (2022)

$$Q(t) = \sum_{i=0}^{4} Q[ds_i|t]P[ds_i|IM] \tag{4}$$

In Eq. (4), $P[ds_i|IM]$ represents the exceedance probability of each damage state as a function of seismic intensity, which can be obtained from the seismic fragility curve. $Q[ds_i|t]$ represents the temporal evolution of a structure's functionality, as defined by the seismic restoration curve.

The functionality loss curve is obtained using Eq. (4) suggested by Huang *et al.* (2022). In this step, the fragility curve and the restoration curve for the same damage state are combined. Eqs. (5) to (7) are then used to describe how the probability of damage is linked to the recovery process. The damage states are classified into five categories, consistent with those defined in the seismic fragility curve: none (ds_0), minor state (ds_1), moderate state (ds_2), extensive state (ds_3), and complete state (ds_4). The seismic functionality loss curves for bridges under different seismic intensities are illustrated in Fig. 4.

The seismic functionality loss curve represents the degree of degradation in structural functionality as a function of seismic intensity. This curve provides an essential indicator for evaluating not only the functionality of individual structures but also the overall loss of functionality across the entire railway network in seismic resilience assessments.

$$P[ds_i|IM] = 1 - P[ds > ds_{i+1}|IM], \quad when\ i = 0 \tag{5}$$

$$P[ds_j|IM] = P[ds > ds_j|IM] - P[ds > ds_{j+1}|IM], \quad when\ j = 1,2,3 \tag{6}$$

$$P[ds_k|IM] = P[ds > ds_k|IM], \quad when\ k = 4 \tag{7}$$

To evaluate the functionality loss of railway structure components, it is first necessary to define the restoration assessment period (t_f) for each structure. Defining the restoration assessment period involves establishing a target timeframe within which the structure is expected to return to its original state. It represents the period following an earthquake during which the recovery of structural functionality is evaluated. Setting an appropriate restoration evaluation period is crucial for realistically reflecting the functionality recovery capacity of the railway network. Therefore, the restoration evaluation period should not simply be based on the total time required for complete recovery but should instead be established according to a realistic disaster response objective. FEMA (2024) proposed recovery rates for bridges, embankments, and tunnels over a total period of 90 days, reporting that most recovery, excluding the complete damage state, is achieved within this timeframe. Accordingly, in this study, the restoration evaluation period was conservatively set to 100 days, considering it as a target time point by which recovery from most damage states could be achieved. The restoration evaluation period was set to 100 days, based on the table

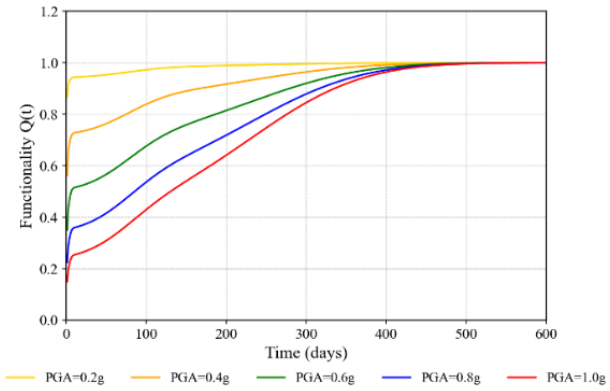

Fig. 4 Seismic functionality curve for bridge

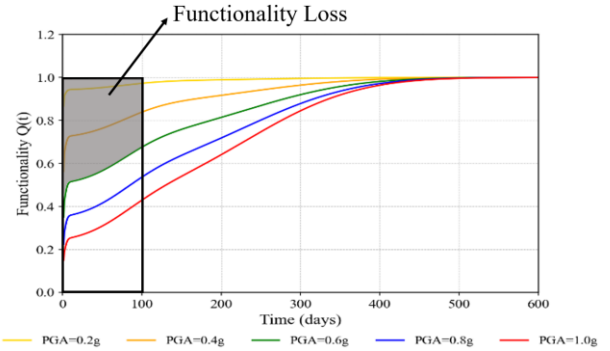

Fig. 5 Schematic drawing of seismic functionality loss

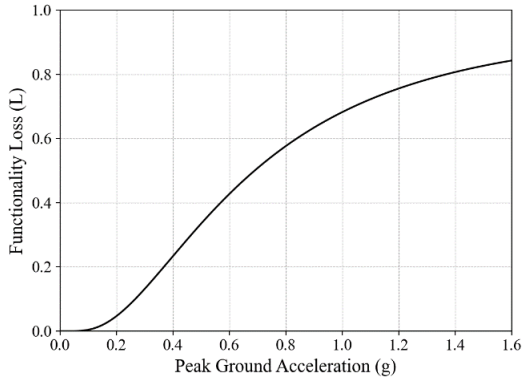

(a) Bridge

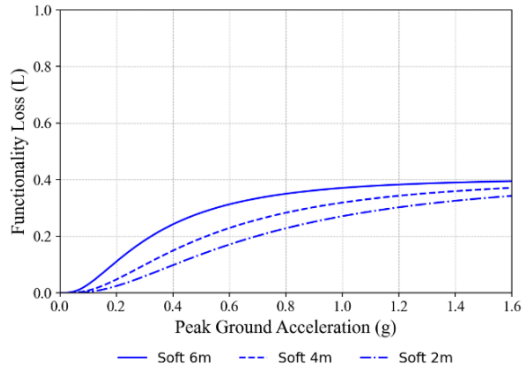

(b) Soft Embankment

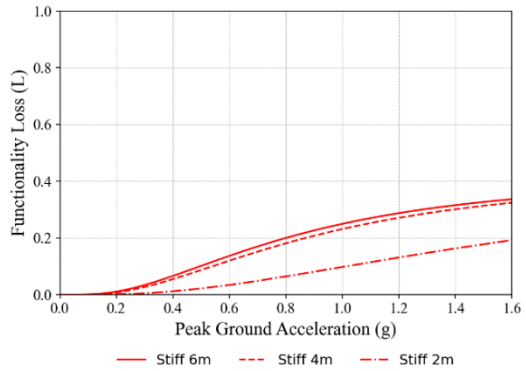

(c) Stiff Embankment

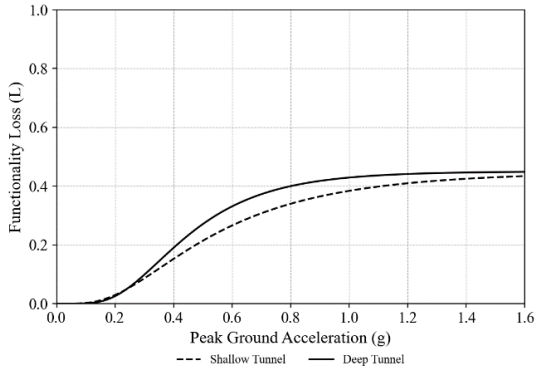

(d) Tunnel

Fig. 6 Seismic functionality loss curve for railway structure

presented by FEMA (2024), as it was considered a reasonable timeframe within which structural components could be sufficiently restored. The functionality loss of each structural component is calculated using Eq. (8), where t_f denotes the restoration evaluation period and t_0 represents the time of earthquake occurrence.

$$Functionality\ Loss\ (L) = 1 - \frac{\int_{t_0}^{t_f} Q(t)}{t_f - t_0} \tag{8}$$

When PGA = 0.6g, the area representing the functionality loss of the bridge is visualized in Fig. 5. The areas corresponding to the functionality loss of each structure were calculated using Eq. (8), and the seismic functionality loss curves for railway structural components, including bridges, embankments, and tunnels, were derived accordingly, as illustrated in Figs. 6(a)-6(d).

2.3 Transportation volume loss prediction for railway network

This study proposed a hypothetical railway network and estimated the transportation volume for each structural component using the OD matrix and station-specific boarding and alighting data.

In addition, the functionality loss of railway structural components of bridges, embankments and tunnels was evaluated based on site-specific ground characteristics (ground classification, amplification factors) and actual distances from the epicenter. The derived functionality losses were used to calculate both the average and maximum functionality losses, which in turn were applied to estimate the transportation volume for each railway line within the network.

The transportation loss based on average functionality loss has the advantage of providing more accurate results by reflecting the functionality loss per kilometer. However, it may underestimate structural components that experience excessive functionality degradation.

On the other hand, the transportation loss based on maximum functionality loss may overestimate components with minor damage, but it allows for a more conservative assessment, enabling better preparedness for extreme disaster scenarios.

2.3.1 Determination of average functionality loss

The average functionality loss for specific sections was estimated by reflecting both the functionality loss of individual structural components and the corresponding line lengths within the simulated railway network. The method of estimating transportation loss using average functionality loss enables a more accurate assessment, as it incorporates segment length data. The transportation loss prediction method based on average functionality loss utilizes line length data and enables precise estimation of loss per kilometer rather than only between stations.

The calculation of transportation loss based on average functionality loss represents the simplest form of proportional distribution using the OD matrix. This method is widely used in practice and serves as a foundational approach, offering the advantage of high reliability.

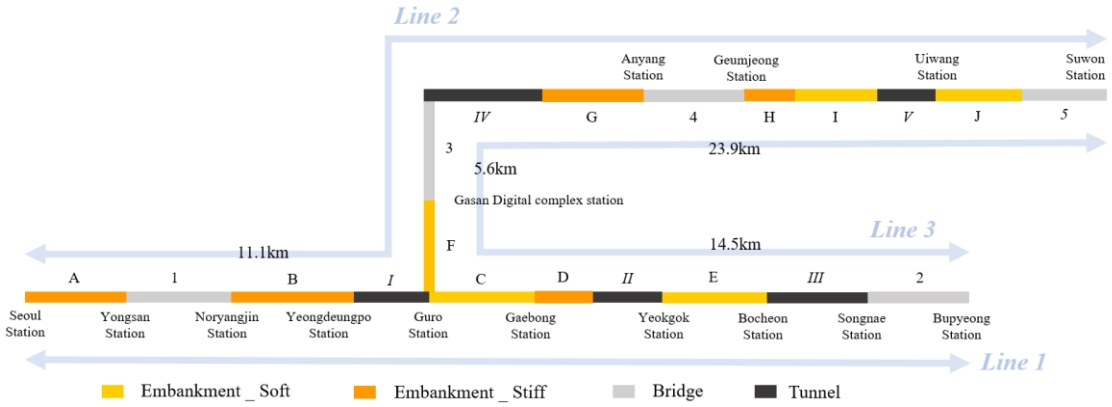

Fig. 7 Railway network for an earthquake scenario

When an earthquake occurs, average functionality matrices were constructed for each railway line and integrated into the OD matrix to estimate the transportation volume for each structural component in the network. The average functionality loss is derived from the functionality loss and the segment length of structural components using the following formula

$$Average\ Functionality\ Loss = \frac{\sum(Distance \times Functionality\ Loss)}{\sum Distance} \quad (9)$$

2.3.2 Determination of maximum functionality loss

When evaluating the transportation volume of the railway network based on average functionality loss, there is a risk that severe functionality losses in some critical structural components may be underestimated due to the averaging process. Accordingly, this study adopted a more conservative approach by considering the maximum functionality loss to quantitatively assess the transportation loss. When evaluating transportation loss between three stations, the highest seismic functionality loss among the two railway structural components located between the stations was selected and assumed to represent the overall functionality loss for that section.

As an example, under an earthquake with magnitude $M_L = 6$, assume a line consisting of Seoul station, Yongsan station, and Noryangjin station. If the seismic functionality loss between Seoul station and Yongsan station is 0.48%, and that between Yongsan station and Noryangjin station is 11.31%, the seismic functionality loss for the entire line is assumed to be represented by the higher value, 11.31%.

Evaluating transportation volume based on the maximum functionality loss allows for the assumption of a worst-case scenario in the event of a disaster. This provides the benefit of facilitating pre-disaster preparedness, which can help minimize potential losses.

3. Application to a simulated railway network

3.1 Transportation volume prediction for simulated railway network

The transportation volume of the simulated railway network was estimated using the boarding and alighting data of Seoul Subway Line 1 and the OD matrix. The simulated railway network was constructed by partially modifying the original model of Subway Line 1. During the development of the railway network inter-station distances were based on real-world measurements and certain stations were omitted to reduce computational complexity and enhance analytical efficiency. The simulated railway network is shown in Fig. 7 and consists of three lines. Line 1 is defined as the route from Seoul to Bupyeong, Line 2 as the route from Seoul to Suwon, and Line 3 as the route from Bupyeong to Suwon.

Table 5 Characteristics of structural components of railway networks

Label	Length	Soil Classification	Structural Characteristics (Embankment height / Tunnel depth)
Bridge. 1	2.8	S2	-
Bridge. 2	2.5	S3	-
Bridge. 3	3.0	S4	-
Bridge. 4	3.8	S4	-
Bridge. 5	3.0	S5	-
Embankment. A	2.8	S2	2
Embankment. B	3.1	S4	4
Embankment. C	2.4	S3	6
Embankment. D	2.0	S5	2
Embankment. E	2.6	S2	4
Embankment. F	2.6	S3	6
Embankment. G	3.2	S4	2
Embankment. H	1.8	S5	4
Embankment. I	2.3	S3	4
Embankment. J	4.7	S4	6
Tunnel. I	2.4	S3	Shallow
Tunnel. II	2.3	S3	Deep
Tunnel. III	2.7	S2	Shallow
Tunnel. IV	3.3	S3	Deep
Tunnel. V	1.8	S2	Deep

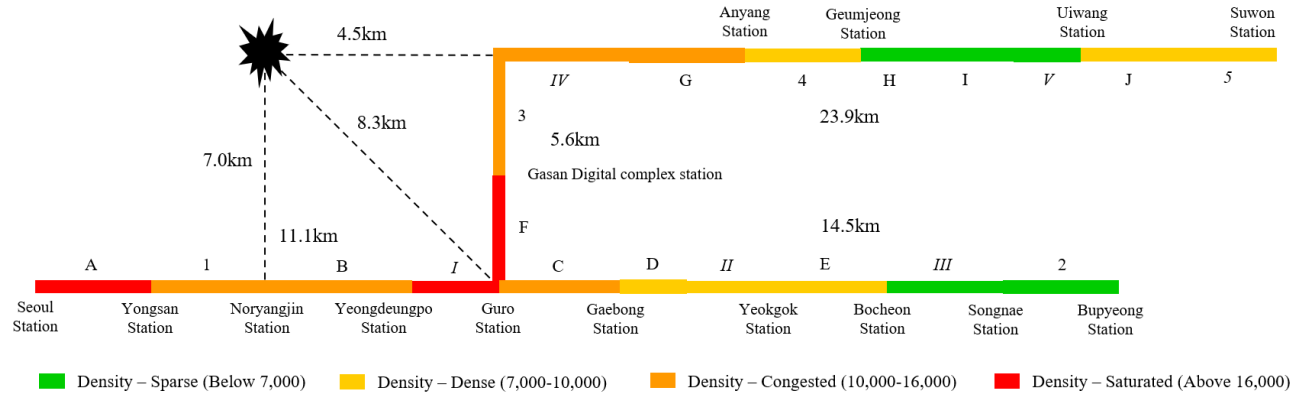

Fig. 8 Density of railway structure

Table 6 Number of boarding and alighting passengers by station on Line 1, data: Seoul Open Data Plaza (2024)

	Seoul	Yongsan	Noryangjin	Yeongdeungpo	Guro	Gaebong	Yeokgok	Bucheon	Songnae	Bupyeong
Boarding	117218	62034	57140	62848	83194	53917	49880	45099	40919	41741
Alighting	119392	63667	56180	62662	83512	54812	47512	45718	39849	44354

Table 7 Transportation volume of Line 1 based on OD Matrix (Normal State)

Boarding \ Alighting	Seoul	Yongsan	Noryangjin	Yeongdeungpo	Guro	Gaebong	Yeokgok	Bucheon	Songnae	Bupyeong
Seoul	-	12082.6	10661.7	11891.9	15848.8	10402.1	9016.7	8676.3	7562.5	8417.4
Yongsan	11991.0	-	5642.4	6293.4	8387.5	5505.0	4771.8	4591.7	4002.2	4454.7
Noryangjin	11045.0	5889.9	-	5796.9	7725.8	5070.7	4395.4	4229.4	3686.5	4103.2
Yeongdeungpo	12148.4	6478.3	5716.4	-	8497.5	5577.2	4834.4	4651.9	4054.7	4513.1
Guro	16081.2	8575.5	7567.0	8440.1	-	7382.8	6399.5	6157.9	5367.4	5974.2
Gaebong	10422.0	5557.7	4904.1	5469.9	7290.0	-	4147.4	3990.8	3478.5	3871.8
Yeokgok	9641.7	5141.5	4536.9	5060.4	6744.2	4426.4	-	3692.0	3218.1	3581.9
Bucheon	8717.5	4648.7	4102.0	4575.3	6097.7	4002.2	3469.1	-	2909.6	3238.6
Songnae	7909.6	4217.9	3721.8	4151.3	5532.6	3631.2	3147.6	3028.8	-	2938.4
Bupyeong	8068.4	4302.6	3796.6	4234.7	5643.7	3704.2	3210.8	3089.6	2693.0	-

The soil classifications and structural characteristics of the railway network's structural components, such as embankment height and tunnel depth, were arbitrarily assumed, while the length of each component was determined based on actual measurements. Detailed information is provided in Table 5. The transportation volume of the railway network, the OD matrix and actual boarding and alighting data from Seoul subway Line 1 were used. The boarding and alighting data for Line 1 of the railway network, provided by Seoul Open Data Plaza. (2024), are presented in Table 6.

The transportation volume of the railway network was estimated using the OD matrix and passenger boarding and alighting data for each railway line. The transportation volume by structural component for Line 1 is presented in Table 7, while the transportation volume for the entire network is illustrated in Fig. 8.

As summarized in Table 8, the total transportation volume by line was as follows: Line 1 carried 544,519 units, representing 31.98% of the overall volume; Line 2 carried 605,896 units (35.58%); and Line 3 carried 552,485 units (32.44%).

3.2 Seismic functionality loss prediction for simulated railway network

3.2.1 Determination of earthquake intensity

This study referenced the 2016 Gyeongju earthquake ($M_L = 5.8$) to establish earthquake conditions suitable for the Korean Peninsula. Using this reference event, the bedrock acceleration for each railway structural component was estimated to derive its seismic functionality loss. In addition, to account for both typical and extreme disaster scenarios, functionality loss for each structural component

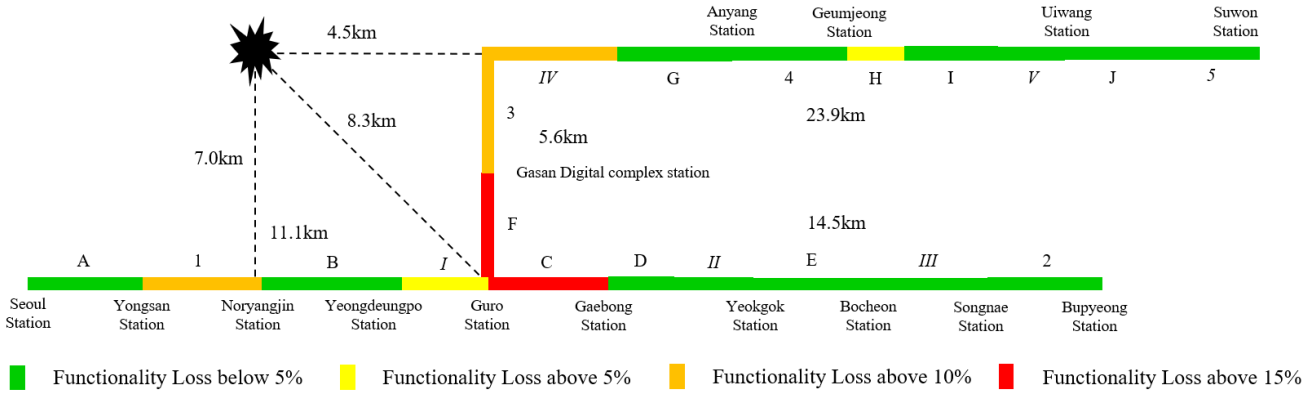

Fig. 9 Functionality loss of the railway network, when $M_L = 6$

Table 9 Detailed Coefficients used in the Ground Motion Attenuation Equation, data: Park *et al*. (1999)

Natural Frequency		ξ_0	ξ_1	ξ_2	ξ_3
a_{max}	C_0	*2.76736*	*0.310489*	*-0.180915E-01*	*0.497951E-02*
	C_1	*-0.434029E-02*	*0.978632E-03*	*-0.228263E-03*	*-0.538469E-05*

Table 8 Transportation Volume of railway network analyzed using OD Matrix

	Transportation Volume	Percentage
Line 1	544,519	31.98 %
Line 2	605,896	35.58 %
Line 3	552,485	32.44 %
Total	1,702,900	

Table 10 Short-period amplification factors, data: KDS 17 10 00 (2024)

Ground Type	$S \leq 0.1$	$S = 0.2$	$S \geq 0.3$
S2	1.4	1.4	1.3
S3	1.7	1.5	1.3
S4	1.6	1.4	1.2
S5	1.8	1.3	1.3

was evaluated under assumed earthquake events with magnitudes $M_L = 6$ and $M_L = 7$. According to Grigoli *et al*. (2018), the focal depths of the Pohang earthquake were reported to range from 3–7 km. In the present study, a conservative assumption of 7 km was adopted.

To estimate the PGA applied to each railway structural component during an earthquake, bedrock acceleration was calculated with reference to the attenuation equation developed for the Korean Peninsula by Park *et al*. (1999). The attenuation equations used in this study are provided in Eqs. (10) and (11), with detailed coefficients listed in Table 9. Deriving the bedrock acceleration for the Korean Peninsula using the following formula. The parameters in Table 9 and Eqs. (10) and (11) are defined as follows: a_{max} is the peak ground acceleration, ξ the attenuation coefficient for the pseudo-velocity response spectra, and R the focal depth (km).

$$log_{10} PGA = C_0 + C_1 R - (log_{10} R) \tag{10}$$

$$C_i = \xi_0^i + \xi_1^i (M_L - 6) + \xi_2^i (M_L - 6)^2 + \xi_3^i (M_L - 6)^3, \quad i = 0, 1 \tag{11}$$

In addition, to account for the effects of site amplification, site amplification factors were applied to estimate the final PGA. To reflect the ground characteristics of the Korean Peninsula, short-period seismic amplification factors from KDS 17 10 00 (2024) were applied. Based on these factors, the final PGA for each structural component was determined for each case. The short-period amplification factors used in the calculation of the final PGA are presented in Table 10.

3.2.2 Determination of functionality loss for structure component: Case 1 ($M_L = 6$)

Using the attenuation equation, the bedrock acceleration was estimated for each structural component within the railway network. Then, short-period amplification factors were applied to derive the final PGA values for each railway structural component. Based on the derived PGA values, Eq. (2) was applied to develop the seismic fragility curves, while the restoration curves for the railway structural components were obtained using Eq. (3).

Subsequently, the two curves were used to derive the functionality curves through Eqs. (4)-(7), and the functionality loss curves for each railway structural component were finally obtained using Eq. (8). Based on these results, the functionality loss of each railway line within the network was evaluated.

When the earthquake magnitude was set to $M_L = 6$, the functionality loss of each structure component within the railway network was derived, as presented in Table 11. This analysis enabled the evaluation of the functionality vulnerability of the railway network and the identification of the most functionally vulnerable structural components.

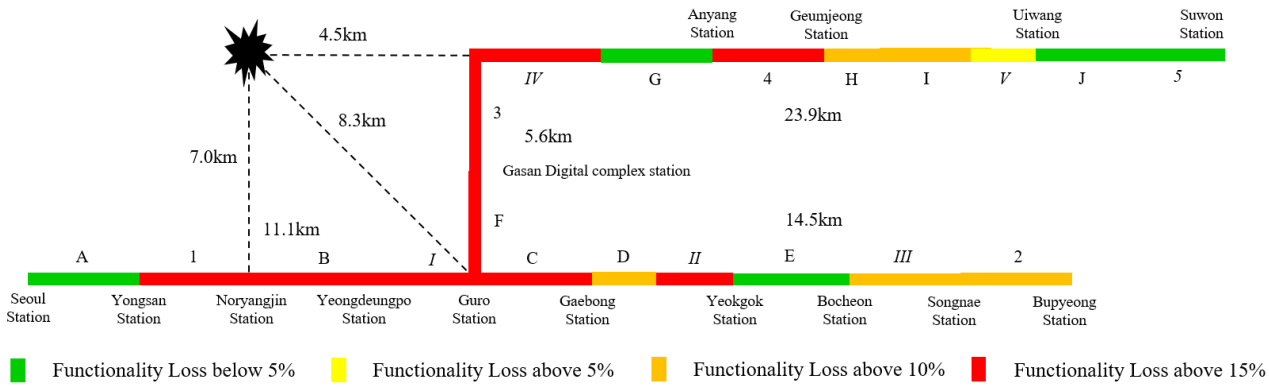

Fig. 10 Functionality loss of the railway network, when $M_L = 7$

Table 11 PGA value and functionality loss value in each structure component, when $M_L = 6$

Label	Length	Distance from Epicenter	Soil Classification	PGA (g)	Height	Functionality Loss
Bridge. 1	2.8	9.97	S2	0.3165	-	11.31%
Bridge. 2	2.5	21.38	S3	0.1666	-	1.16%
Bridge. 3	3.0	8.45	S4	0.3446	-	13.90%
Bridge. 4	3.8	14.68	S4	0.2262	-	4.03%
Bridge. 5	3.0	27.80	S5	0.1285	-	0.33%
Embankment. A	2.8	10.71	S2	0.2965	2	0.48%
Embankment. B	3.1	7.66	S4	0.3686	4	4.52%
Embankment. C	2.4	12.07	S3	0.2862	6	17.59%
Embankment. D	2.0	13.45	S5	0.2444	2	3.83%
Embankment. E	2.6	16.90	S2	0.1802	4	0.55%
Embankment. F	2.6	9.36	S3	0.3477	6	21.45%
Embankment. G	3.2	11.72	S4	0.2738	2	0.37%
Embankment. H	1.8	17.19	S5	0.2107	4	5.23%
Embankment. I	2.3	19.08	S3	0.1876	4	4.10%
Embankment. J	4.7	24.09	S4	0.1360	6	0.28%
Tunnel. I	2.4	10.87	S3	0.3113	Shallow	9.32%
Tunnel. II	2.3	14.99	S3	0.2367	Deep	4.73%
Tunnel. III	2.7	19.12	S2	0.1563	Shallow	1.28%
Tunnel. IV	3.3	9.32	S3	0.3489	Deep	14.30%
Tunnel. V	1.8	21.00	S2	0.1401	Deep	0.51%

Based on the functionality loss derived for each railway structural component, the severity of functionality loss was categorized into four ranges: less than 5%, 5% to less than 10%, 10% to less than 15%, and 15% or more.

When an $M_L = 6$ earthquake occurs, the sections between Guro station and Gaebong station, and between Guro station and Gasan Digital Complex station are identified as the most functionally degraded and logistically constrained segments within the railway network. These two segments account for 2 out of the 20 total sections. The corresponding results are illustrated in Fig. 9.

3.2.3 Determination of functionality loss for structure component: Case 2 ($M_L = 7$)

When the earthquake magnitude was set to $M_L = 7$, the functionality loss of each structure component within the railway network was derived, as presented in Table 12. This analysis enabled the evaluation of the functionality vulnerability of the railway network and the identification of the most functionally vulnerable structural components.

The functionality loss of each railway structural component was categorized into four levels, following the same classification used for the $M_L = 6$ earthquake scenario. When an $M_L = 7$ earthquake occurs, the most functionally degraded and logistically constrained segments in the railway network are identified as the sections from Yongsan station to Gaebong station, partial segments from Gaebong station to Yeokgok station, from Guro station to

Table 12 PGA value and functionality loss value in each structure component, when $M_L = 7$

Label	Length	Distance from Epicenter	Soil Classification	PGA (g)	Height	Functionality Loss
Bridge. 1	2.8	9.97	S2	0.6260	-	34.32%
Bridge. 2	2.5	21.38	S3	0.3049	-	10.26%
Bridge. 3	3.0	8.45	S4	0.6900	-	36.89%
Bridge. 4	3.8	14.68	S4	0.3777	-	16.96%
Bridge. 5	3.0	27.80	S5	0.2319	-	4.40%
Embankment. A	2.8	10.71	S2	0.5791	2	3.13%
Embankment. B	3.1	7.66	S4	0.7670	4	17.14%
Embankment. C	2.4	12.07	S3	0.5084	6	28.60%
Embankment. D	2.0	13.45	S5	0.4512	2	11.75%
Embankment. E	2.6	16.90	S2	0.3574	4	4.20%
Embankment. F	2.6	9.36	S3	0.6698	6	32.85%
Embankment. G	3.2	11.72	S4	0.4846	2	2.00%
Embankment. H	1.8	17.19	S5	0.3422	4	12.06%
Embankment. I	2.3	19.08	S3	0.3346	4	11.67%
Embankment. J	4.7	24.09	S4	0.2565	6	2.23%
Tunnel. I	2.4	10.87	S3	0.5698	Shallow	25.12%
Tunnel. II	2.3	14.99	S3	0.3997	Deep	18.96%
Tunnel. III	2.7	19.12	S2	0.3262	Shallow	10.30%
Tunnel. IV	3.3	9.32	S3	0.6734	Deep	36.29%
Tunnel. V	1.8	21.00	S2	0.2905	Deep	8.98%

Table 13 Average functionality loss rate of Line 1 in the railway network (Case 1: $M_L = 6$)

Boarding \ Alighting	Seoul	Yongsan	Noryangjin	Yeongdeungpo	Guro	Gaebong	Yeokgok	Bucheon	Songnae	Bupyeong
Seoul	-	0.48	5.89	5.40	6.25	8.26	7.31	6.45	5.84	5.39
Yongsan	0.48	-	11.31	7.74	8.20	10.30	8.58	7.40	6.58	5.99
Noryangjin	5.89	11.31	-	4.52	6.61	9.95	7.96	6.66	5.83	5.24
Yeongdeungpo	5.40	7.74	4.52	-	9.32	13.45	9.13	7.22	6.11	5.38
Guro	6.25	8.20	6.61	9.32	-	17.59	9.07	6.69	5.47	4.73
Gaebong	8.26	10.30	9.95	13.45	17.59	-	4.31	2.89	2.44	2.17
Yeokgok	7.31	8.58	7.96	9.13	9.07	4.31	-	0.55	0.92	1.00
Bucheon	6.45	7.40	6.66	7.22	6.69	2.89	0.55	-	1.28	1.22
Songnae	5.84	6.58	5.83	6.11	5.47	2.44	0.92	1.28	-	1.16
Bupyeong	5.39	5.99	5.24	8.38	4.73	2.17	1.00	1.22	1.16	-

Anyang station, and the segment between Anyang station and Geumjeong station. These account for 9 out of the 20 total segments. The corresponding results are visualized in Fig. 10.

3.3 Transportation volume loss prediction for simulated railway network

3.3.1 Average functionality loss

Based on the functionality loss of railway structural components for each earthquake magnitude, the average functionality loss for specific segments was calculated for $M_L = 6$ and $M_L = 7$ using Eq. (8) and the corresponding lengths of each component. First, the average functionality loss of the railway network was calculated for an earthquake with magnitude $M_L = 6$. As a result, the functionality loss of a given segment was represented by the average functionality loss of the structural components within that segment.

For example, if the functionality loss of the structural components between Yeongdeungpo station and Guro station is 9.32%, and that between Guro station and Gaebong station is 17.59%, then using the average functionality loss approach, the functionality loss for the entire segment from Yeongdeungpo to Gaebong station would be represented as 13.45%. Using this approach, the

Table 14 Average functionality loss rate of Line 1 in the railway network (Case 2: $M_L = 7$)

Boarding \ Alighting	Seoul	Yongsan	Noryangjin	Yeongdeungpo	Guro	Gaebong	Yeokgok	Bucheon	Songnae	Bupyeong
Seoul	-	3.13	18.73	18.16	19.67	21.26	19.89	17.89	17.00	16.34
Yongsan	3.13	-	34.32	25.30	25.25	26.00	23.02	20.24	18.92	17.97
Noryangjin	18.73	34.32	-	17.14	20.63	23.05	20.43	17.57	16.45	15.68
Yeongdeungpo	18.16	25.30	17.14	-	25.12	26.86	21.54	17.69	16.30	15.41
Guro	19.67	25.25	20.63	25.12	-	28.60	20.26	15.77	14.54	13.80
Gaebong	21.26	26.00	23.05	26.83	28.60	-	15.61	11.31	11.02	10.87
Yeokgok	19.89	23.02	20.43	24.54	20.26	15.61	-	4.20	7.31	8.25
Bucheon	17.89	20.24	17.57	17.69	15.77	11.31	4.20	-	10.30	10.28
Songnae	17.00	18.92	16.45	16.30	14.54	11.02	7.31	10.30	-	10.26
Bupyeong	16.34	17.97	15.68	15.41	13.80	10.87	8.25	10.28	10.26	-

Table 15 Maximum functionality loss rate of Line 1 in the railway network (Case 1: $M_L = 6$).

Boarding \ Alighting	Seoul	Yongsan	Noryangjin	Yeongdeungpo	Guro	Gaebong	Yeokgok	Bucheon	Songnae	Bupyeong
Seoul	-	0.48	11.31	11.31	11.31	17.59	17.59	17.59	17.59	17.59
Yongsan	0.48	-	11.31	11.31	11.31	17.59	17.59	17.59	17.59	17.59
Noryangjin	11.31	11.31	-	4.52	9.32	17.59	17.59	17.59	17.59	17.59
Yeongdeungpo	11.31	11.31	4.52	-	9.32	17.59	17.59	17.59	17.59	17.59
Guro	11.31	11.31	9.32	9.32	-	17.59	17.59	17.59	17.59	17.59
Gaebong	17.59	17.59	17.59	17.59	17.59	-	4.73	4.73	4.73	4.73
Yeokgok	17.59	17.59	17.59	17.59	17.59	4.73	-	0.55	1.28	1.28
Bucheon	17.59	17.59	17.59	17.59	17.59	4.73	0.55	-	1.28	1.28
Songnae	17.59	17.59	17.59	17.59	17.59	4.73	1.28	1.28	-	1.16
Bupyeong	17.59	17.59	17.59	17.59	17.59	4.73	1.28	1.28	1.16	-

overall average functionality loss of the railway network was derived. For $M_L = 6$, Table 13 presents the segment-wise average functionality loss of Line 1 in the railway network.

The average functionality loss of the railway network under an $M_L = 7$ earthquake was derived using the same approach as that applied for the $M_L = 6$ scenario. As a result, the average functionality loss between Seoul station and Guro station under an $M_L = 7$ earthquake was approximately 3.14 times higher than that under an $M_L = 6$ earthquake. The average functionality loss for Line 1 of the railway network under an $M_L = 7$ earthquake is presented in Table 14.

3.3.2 Maximum functionality loss

However, when using average functionality loss, there is a risk of underestimating the functionality loss in segments that exhibit excessive or localized damage. Therefore, the maximum functionality loss for $M_L = 6$ was derived by assuming that the highest functionality loss among the railway structural components within a given segment represents the functionality loss of that segment. As a result, in some cases, structural components that would otherwise be considered functionally sound under seismic loading may be conservatively assessed as experiencing excessive functionality loss. For example, if a specific segment is defined by one station located between Seoul station and Guro station and another station located between Gaebong station and Bupyeong station, the functionality loss for that segment is assumed to be 17.59%, which corresponds to the highest functionality loss observed on Line 1. Using this method, the maximum functionality loss for Line 1 in the railway network was estimated, as shown in Table 15.

As with the $M_L = 6$ scenario, the maximum functionality loss of the railway network was derived for the $M_L = 7$ earthquake. As a result, the maximum functionality loss between Seoul station and Bupyeong station under an $M_L = 7$ earthquake was found to be 1.95 times higher than that under an $M_L = 6$ earthquake. The maximum functionality loss for Line 1 of the railway network under an $M_L = 7$ earthquake is presented in Table 16.

3.4 Summary of transportation volume loss

Finally, the average and maximum functionality losses for all railway lines were derived for both $M_L = 6$ and $M_L = 7$ earthquake scenarios. The average functionality losses of the railway network for $M_L = 6$ and $M_L = 7$ earthquakes are summarized in Table 17.

In the case of an earthquake with magnitude $M_L = 6$, the transportation loss rates for Line 1, Line 2, and Line 3 were found to be 6.52%, 8.20%, and 8.17%, respectively.

Table 16 Maximum functionality loss rate of Line 1 in the railway network (Case 2: $M_L = 7$)

Alighting / Boarding	Seoul	Yongsan	Noryangjin	Yeongdeungpo	Guro	Gaebong	Yeokgok	Bucheon	Songnae	Bupyeong
Seoul	-	3.13	34.32	34.32	34.32	34.32	34.32	34.32	34.32	34.32
Yongsan	3.13	-	34.32	34.32	34.32	34.32	34.32	34.32	34.32	34.32
Noryangjin	34.32	34.32	-	17.14	25.12	28.60	28.60	28.60	28.60	28.60
Yeongdeungpo	34.32	34.32	17.14	-	25.12	28.60	28.60	28.60	28.60	28.60
Guro	34.32	34.32	25.12	25.12	-	28.60	28.60	28.60	28.60	28.60
Gaebong	34.32	34.32	28.60	28.60	28.60	-	18.96	18.96	18.96	18.96
Yeokgok	34.32	34.32	28.60	28.60	28.60	18.96	-	4.20	10.30	10.30
Bucheon	34.32	34.32	28.60	28.60	28.60	18.96	4.20	-	10.30	10.30
Songnae	34.32	34.32	28.60	28.60	28.60	18.96	10.30	10.30	-	10.26
Bupyeong	34.32	34.32	28.60	28.60	28.60	18.96	10.30	10.30	10.26	-

Table 17 Transportation volume reflecting Average functionality loss of the railway network

(a) Case 1. $M_L = 6$

	Transportation Volume (Normal State)	Transportation Volume Loss	Percentage
Line 1	544,519	35,502	6.52%
Line 2	605,896	49,681	8.20%
Line 3	552,485	45,133	8.17%
Total	1,702,900	130,316	7.65%

(b) Case 1. $M_L = 7$

	Transportation Volume (Normal State)	Transportation Volume Loss	Percentage
Line 1	544,519	99,769	18.32%
Line 2	605,896	126,277	20.84%
Line 3	552,485	103,848	18.80%
Total	1,702,900	329,894	19.37%

Table 18 Transportation volume reflecting Maximum functionality loss of the railway network

(a) Case 1. $M_L = 6$

	Transportation Volume (Normal State)	Transportation Volume Loss	Percentage
Line 1	544,519	69,708	12.80%
Line 2	605,896	97,861	16.15%
Line 3	552,485	90,048	16.30%
Total	1,702,900	257,617	15.13%

(b) Case 1. $M_L = 7$

	Transportation Volume (Normal State)	Transportation Volume Loss	Percentage
Line 1	544,519	151,302	27.79%
Line 2	605,896	194,194	32.05%
Line 3	552,485	167,802	30.37%
Total	1,702,900	513,298	30.14%

The average transportation loss rate across the entire railway network was analyzed to be 7.65%. In the case of an earthquake with magnitude $M_L = 7$, the transportation loss rates for Line 1, Line 2, and Line 3 were found to be 18.32%, 20.84%, and 18.80%, respectively. The average transportation loss rate across the entire railway network was analyzed to be 19.37%.

Next, the maximum functionality losses of the railway network for $M_L = 6$ and $M_L = 7$ earthquakes are summarized in Table 18.

In the case of an earthquake with magnitude $M_L = 6$, the transportation loss rates were 12.80% for Line 1, 16.15% for Line 2, and 16.30% for Line 3. The average transportation loss rate across the entire railway network was calculated to be 15.13%, which is approximately 1.8 to 2 times higher than the transportation loss estimated using average functionality loss. In the case of an earthquake with magnitude $M_L = 7$, the transportation loss rates were found to be 27.79% for Line 1, 32.05% for Line 2, and 30.37% for Line 3. The average transportation loss rate across the entire railway network was 30.14%, which is approximately 1.5 times higher than the transportation loss estimated based on average functionality loss.

4. Discussion

This study quantitatively assessed the transportation loss experienced by the railway network's bridges, embankments and tunnels during an earthquake. First, the transportation volume between stations within the railway network was quantitatively analyzed using the OD matrix and station-specific boarding and alighting data. Subsequently, functionality loss for each structural component in the railway network was assessed using the functionality and functionality loss curves obtained by combining seismic fragility and restoration curves. Finally, the method was proposed to quantitatively evaluate the transportation loss of the entire railway network by integrating transportation analysis with functionality loss results.

The proposed methodology was applied to a hypothetical railway network under earthquake scenarios to evaluate the potential transportation loss that could realistically occur.

To estimate the overall transportation volume of the simulated railway network, an OD matrix was constructed using actual boarding and alighting data from each station of Seoul Subway Line 1. This allowed for the quantitative evaluation of transportation volume between stations and the identification of areas with concentrated transportation

demand. While the simulated railway network reflects real-world track configurations, some stations were omitted to ensure computational efficiency, as the study primarily aims to present the methodological approach. Furthermore, the railway network was segmented into Line 1, Line 2, and Line 3, and the transportation volume was calculated for each line individually.

To evaluate the transportation loss in the railway network, it is first necessary to derive the functionality loss curves for each structural component. Functionality loss curves for the railway structural components were developed using the seismic fragility curves and restoration curves corresponding to each component.

First, the seismic fragility function for railway bridges was based on the study by Kim *et al*. (2023), while the fragility function for embankment sections was developed with reference to the research on embankments and cut slopes by Argyroudis and Kaynia (2015). For tunnel sections, the nonlinear dynamic analysis-based seismic fragility curve proposed by Kwon *et al*. (2024) was applied.

Next, restoration curves for railway structural components such as bridges, embankments and tunnels were developed using average recovery times and recovery rates by damage state as reported by Yoo *et al.* (2025). After integrating the derived seismic fragility curves with the restoration curves, the restoration evaluation period was conservatively set to 100 days based on the functional percentages of structural components reported by FEMA (2024). This extension beyond the maximum 90-day criterion suggested by FEMA (2024) was introduced as a safety margin, thereby acknowledging the evidence that most damage states are restored within 90 days while mitigating the associated uncertainties. Furthermore, adopting a unified 100-day evaluation period enables the restoration progress to be quantitatively aligned with the percentage of functionality loss. This provides the advantage of consistently comparing and evaluating the recovery probability for each damage state under a common standard.

In this process, the functionality loss of each railway structural component was evaluated based on the PGA estimated from site classification, embankment height, tunnel depth, epicentral distance, and bedrock acceleration. The transportation loss in the railway network was evaluated by incorporating both average and maximum functionality loss, with the aim of producing more reliable results and providing a basis for conservative response strategies.

The earthquake scenarios were established based on the 2016 Gyeongju earthquake ($M_L = 5.8$), a past seismic event in the Korean Peninsula. Considering the maximum earthquake intensity that could occur in the region, an earthquake of magnitude $M_L = 6$ was set as a realistically possible disaster scenario, while a magnitude $M_L = 7$ was defined as an extreme disaster scenario.

Based on the 2016 Pohang earthquake, the focal depth was set to approximately 7 km. Bedrock acceleration for each railway structural component was derived using its epicentral distance and the attenuation equations developed for the Korean Peninsula by Park *et al*. (1999). Next, the bedrock acceleration values were adjusted using the short-period amplification factors provided in the Korean seismic design standard KDS 17 10 00 (2024), to compute the site-amplified PGA for each railway structural component. The attenuation equations and site amplification factors adopted in this study were developed considering the geological characteristics of the Korean Peninsula, which are consistent with the ground conditions of the railway network components proposed in this study. However, since their application in this research is primarily methodological, more recent research findings may be applied when they become available in the future.

As a result, under an earthquake of magnitude $M_L = 6$, most railway structures exhibited less than 5% functionality loss. However, several sections showed losses of approximately 10–15%. In particular, the Guro–Gaebong and Guro–Gasan Digital Complex sections reached the maximum functionality degradation stage proposed in this study, with functionality losses of approximately 17.59% and 21.45%, respectively.

In contrast, under an extreme earthquake of magnitude $M_L = 7$, functionality loss expanded across the entire railway network. Severe functionality degradation exceeding 15% was observed in 11 sections, including the Yongsan–Yeokgok and Guro–Geumjeong sections. Overall, the network experienced substantially greater functionality losses compared to those under the $M_L = 6$ scenario.

Subsequently, average functionality loss was applied to estimate the transportation loss across the railway network. For an $M_L = 6$ earthquake, the application of average functionality loss led to transportation losses of 6.52%, 8.20%, and 8.17% for Line 1, Line 2, and Line 3, respectively, resulting in an overall loss of about 7.65%. This corresponds to a transportation loss equivalent to 7.65% of the total volume over the 100-day restoration evaluation period, which can be interpreted as a functional disruption of railway transport for approximately 7.65 days during that time frame. For an $M_L = 7$ earthquake, the average functionality losses were 18.32% for Line 1, 20.84% for Line 2, and 18.80% for Line 3. The overall transportation loss across the network was 19.37%, which is approximately 2.53% higher than the loss observed under the $M_L = 6$ scenario. This is equivalent to a loss of railway transport functionality for about 18.8 days over a 100-day period, indicating that significantly greater transportation loss may occur compared to that estimated using average functionality loss.

This study proposes a methodology to quantitatively evaluate the functionality losses of railway networks during seismic events and translate them into transportation losses. Unlike previous studies limited to individual structures, this approach incorporates network-level impacts to provide a more realistic assessment of operational disruptions. For example, by combining freight rates with functionality loss ratios over a 100-day period, the economic losses in freight transport can be estimated, and the loss-cost matrix can be used to identify priority railway segments for restoration.

5. Conclusions

This study proposed a methodology for quantitatively assessing transportation loss caused by earthquakes by incorporating both the average and maximum functionality loss of the railway network.

The transportation loss for each structural component of the simulated railway network was estimated using the OD Matrix and the actual boarding and alighting data from Seoul Subway Line 1. For each structural component of the railway network, the seismic functionality curve and the seismic functionality loss curve were derived by integrating the seismic fragility curve with the seismic restoration curve. The overall transportation loss of the simulated railway network was estimated by combining the average functionality loss method and the maximum functionality loss method, both of which were applied based on the derived transportation loss and functionality loss for each structural component. Furthermore, the proposed approach was applied to the simulated railway network to evaluate its applicability.

When the analysis was conducted based on the maximum functionality loss, it was found that under an earthquake with a magnitude of $M_L = 6$, the transportation loss rates were 12.80% for Line 1, 16.15% for Line 2, and 16.30% for Line 3, with an overall transportation loss rate of 15.13%. Under an earthquake with a magnitude of $M_L = 7$, the transportation loss rates increased to 27.79% for Line 1, 32.05% for Line 2, and 30.37% for Line 3, resulting in an overall transportation loss rate of 31.14%. This indicates that the transportation losses could be 1.5 to 2 times greater compared to those based on the average functionality loss, highlighting the risk that responding based solely on average functionality loss in actual disaster situations may significantly underestimate potential losses.

The proposed methodology enables the pre-disaster identification of functionality loss for individual components within the railway network and allows for the quantitative prediction of transportation losses by incorporating this information. By identifying the segments with the most severe functionality degradation, the proposed methodology supports the prioritization of recovery efforts, thereby helping to minimize overall transportation loss and accelerate the restoration of the railway network. The methodology proposed in this study provides a practical foundation for establishing effective and structured disaster recovery strategies and is anticipated to enhance the seismic resilience of the railway network.

However, this study proposes a novel methodology that differs from existing literature, and thus requires further validation through comparative analysis with both actual transportation disruptions caused by real seismic events and results from previous studies. Accordingly, future research will focus on validating and enhancing the proposed model by conducting comparative assessments with empirical case studies and established methodologies.

Acknowledgments

This research was supported by a grant from R&D Program (PK2502A2) of the Korea Railroad Research Institute.

References

Andreotti, G. and Lai, C.G. (2019), "Use of fragility curves to assess the seismic vulnerability in the risk analysis of mountain tunnels", *Tunn. Undergr. Sp. Tech.*, **91**, 103008. https://doi.org/10.1016/j.tust.2019.103008.

Argyroudis, S. and Kaynia, A.M. (2015), "Analytical seismic fragility functions for highway and railway embankments and cuts", *Earthq. Eng. Struct. D.*, **44**(11), 1863-1879. https://doi.org/10.1002/eqe.2563.

Avanaki, M.J., Hoseini, A., Vahdani, S., de Santos, C. and de la Fuente, A. (2018), "Seismic fragility curves for vulnerability assessment of steel fiber reinforced concrete segmental tunnel linings", *Tunn. Undergr. Sp. Tech.,* **78**, 259-274. https://doi.org/10.1016/j.tust.2018.04.032.

Cho, S.K. (2008), "A study on synthetic OD Estimation Model based on Partial Traffic Volumes and User-Equilibrium Information", *J. Korea Inst. Intell. Transp. Syst*, **7**(5), 180-183.

Guo, W., Hu, Y., Liu, H. and Bu, D. (2019), "Seismic performance evaluation of typical piers of China's high-speed railway bridge line using pushover analysis", *Math. Probl. Eng.*, **2019**(1), 9514769. https://doi.org/10.1155/2019/9514769.

Grigoli, F., Cesca, S., Rinaldi, A.P., Manconi, A., López-Comino, J.A., Clinton, J.F., Westaway, R., Cauzzi, C., Dahm, T. and Wiemer, S. (2018), "The November 2017 M_w 5.5 Pohang earthquake: A possible case of induced seismicity in South Korea", *Science*, **360**(6392), 1003-1006. https://doi.org/10.1126/science.aat2010

Huang, Z., Zhang, D., Pitilakis, K., Tsinidis, G., Huang, H., Zhang, D. and Argyroudis, S. (2022), "Resilience assessment of tunnels: Framework and application for tunnels in alluvial deposits exposed to seismic hazard", *Soil Dyn. Earthq. Eng.*, **162**, 107456. https://doi.org/10.1016/j.soildyn.2022.107456.

Kim, J., Kim, H., Yoo, M. and Ha, I. (2023), "Research on development and application of earthquake risk assessment model for railway structures", *J. Korean Soc. Railway*, **26**(9), 652–663. 10.7782/JKSR.2023.26.9.652

Kwon, S.Y., Yoo, M. and Hong, S. (2020), "Earthquake risk assessment of underground railway station by fragility analysis based on numerical simulation", *Geomech. Eng.*, **21**(2), 143-152. https://doi.org/10.12989/gae.2020.21.2.143.

Kwon, S.Y., Kim, J., Kwak, D., Yang, S. and Yoo, M. (2024), "Development of seismic fragility function for underground railway station structures in Korea", *Buildings*, **14**(5), 1200. https://doi.org/10.3390/buildings14051200.

Lee, S.I. and Lee, S.Y. (2023), "Exploring spatiotemporal dynamics of the impact of migration on population redistribution: A case study of internal migration in South Korea", *J. Korean Cartogr. Assoc.*, **23**(1), 1-19. https://doi.org/10.16879/jkca.2023.23.1.001.

Liu, N., Huang, Q.B., Fan, W., Ma, Y.J. and Peng, J.B. (2018), "Seismic responses of a metro tunnel in a ground fissure site", *Geomech. Eng.*, **15**(2), 775-781. https://doi.org/10.12989/gae.2018.15.2.775.

Nguyen, D.D., Park, D., Shamsher, S., Nguyen, V.Q. and Lee, T.H. (2019), "Seismic vulnerability assessment of rectangular cut-and-cover subway tunnels", *Tunn. Undergr. Sp. Tech.*, **86**, 247-261. https://doi.org/10.1016/j.tust.2019.01.021.

Park, J.U., Noh, M. and Lee, K. (1999), "Development of attenuation equations of ground motions in the southern part of the Korean peninsula", *J. Earthq. Eng. Soc. Korea*, **3**, 21-27.

Wang, Y., Wang, T. and Tang, Z. (2014), "Seismic fragility of cushioning high-speed railway bridges", *Adv. Transp. Stud., Special Issue 2014*, 39-50. 10.4399/97888548783105.

Wei, B., Yang, T., Jiang, L. and He, X. (2018), "Effects of friction-based fixed bearings on the seismic vulnerability of a high-

speed railway continuous bridge", *Adv. Struct. Eng.*, **21**(5), 643-657. https://doi.org/10.1177/1369433217726894.

Yang, H.J., Nam, H.W. and Jun, C.M. (2018), "Analysing potential improvement of public transit services in OD level using time-distance accessibility and smartcard traffic volume", *J. Korean Assoc. Geogr. Inf. Stud.*, **21**(2), 80-93. https://doi.org/10.11108/kagis.2018.21.2.080

Yang S., Kwak D., Kim, S., Yoo, B. and Yoo, M. (2024), "Evaluation and development of seismic fragility models for cut-and-cover underground station", *J. Koran Soc. Railway*, **27**(3), 202-212. https://doi.org/10.7782/JKSR.2024.27.3.202.

Yang, S., Kwak, D. and Kishida, T. (2020), "Development of seismic fragility curves for high-speed railway system using earthquake case histories", *Geomech. Eng.*, **21**(2), 179-186. https://doi.org/10.12989/gae.2020.21.2.179.

Yoo, M., Jeon, J., Kim, S. and Haam, S. (2025), "Suggestions and applications for evaluating seismic functionality for railway infrastructure network based on fragility curve", *Appl. Sci.*, **15**(2), 534. https://doi.org/10.3390/app15020534.

Yoo, M., Kwon, S.Y. and Hong, S. (2022), "Dynamic response evaluation of deep underground structures based on numerical simulation", *Geomech. Eng.*, **29**(3), 269-279. https://doi.org/10.12989/gae.2022.29.3.269.

Yoo, M. and Hong, S. (2024), "Evaluation of dynamic earth pressure acting on pile foundation in liquefiable sand deposit by shaking table tests", *Geomech. Eng.*, **38**(5), 487-495. https://doi.org/10.12989/gae.2024.38.5.487.

Kurian, S.A., Deb, S.K. and Dutta, A. (2006), "Seismic vulnerability assessment of a railway overbridge using fragility curves", *Proceedings of the 4th International Conference on Earthquake Engineering (4ICEE)*, Taipei, Taiwan, October. https://www.researchgate.net/publication/255599937.

Park, D., Lee, T.H., Nguyen, D.D. and Ahn, J.K. (2019), "Development of fragility curves for underground box tunnels from nonlinear frame analysis", *Earthquake Geotechnical Engineering for Protection and Development of Environment and Constructions.* Rome, Italy, June.

Wei, B., Li, C., Hu, Z., Zhou, Y., Jiang, L. and Li, S. (2020), "Applicability of artificial waves to seismic vulnerability of high-speed Railway Continuous Bridge", *Proceedings of the 2020 Int. Conf. Intell. Transp., Big Data Smart City (ICITBS), IEEE*, Vientiane, Laos, January. 10.1109/ICITBS49701.2020.00026

Federal Emergency Management Agency (2024), *Hazus Earthquake Model Technical Manual, Version 6.1*, Federal Emergency Management Agency, Washington, DC, USA.

Ministry of Land, Infrastructure and Transport (MOLIT). (2024), *KDS 17 10 00:2024 General Structural Design Standards*, Ministry of Land, Infrastructure and Transport, Sejong, Sejong, South Korea.

Seoul Open Data Plaza. (2024), Seoul Open Data Plaza, Seoul, South Korea. Retrieved from https://data.seoul.go.kr/dataList/OA-12914/S/1/datasetView.do#